



UNIVERSIDADE DA BEIRA INTERIOR

Engenharia

Development of a CubeSat power management subsystem for the ALSat#1 Mission

Jorge Antunes Panagopoulos

Dissertação para obtenção do Grau de Mestre em

Engenharia Aeronáutica

(ciclo de estudos integrado)

Orientador: Prof. Doutor Anna Guerman

Co-orientador: Prof. Doutor Franco Bernelli Zazzera

Covilhã, Janeiro de 2020

Acknowledgements

I would like to express my gratitude to Professor Anna Guerman for giving me the opportunity to go to the Politecnico di Milano, her advises and support through the completion of this thesis.

To Professor Franco Bernelli-Zazzera, I am very grateful for accepting me in his research group at the Department of Aerospace Engineering at the Politecnico di Milano and giving me the opportunity to develop this project, for his advises, facilities and continuous support in the completion of this study.

To my colleagues and friends for their help and company through the good years we spent at the Universidade da Beira Interior and, recently, at the Politecnico di Milano and the residence InDomus, I am very thankful.

Finally, I thank my family whose continued support made all this possible.

Abstract

This thesis aims to develop and analyse the power management subsystem for the ALSat#1 mission that studies the cosmic rays in low earth orbit. The primary task is to find components to build and make the CubeSat able to do the mission and subsequently analyse if it is capable to make the mission in three different orbits RAANs (RAAN 0°; RAAN 53.5°; RAAN 90°) with different eclipse times.

This was done by using a MATLAB programme to analyse the energy consumed and energy deficit during an orbit and during a day.

It was found out that the options orbit with RAAN 0° and orbit with RAAN 53.5° can complete the mission without change. However, the orbit with RAAN 90° has some deficit cumulated after a day which leads to energy insufficiency, and is only possible to overcome it with some changes in the algorithm or in the components used.

Keywords

CubeSat, nanosatellites, power management subsystem, cosmic rays, low earth orbit, algorithm, MATLAB.

Resumo

Esta tese tem como objetivo desenvolver e analisar o subsistema de gerenciamento de energia da missão ALSat # 1 que pretende estudar os raios cósmicos em órbita terrestre baixa. A tarefa principal é encontrar componentes para construir e tornar o CubeSat capaz de realizar a missão e, posteriormente, analisar sua capacidade de realizar a missão em três RAANs de órbita diferentes (RAAN 0°; RAAN 53,5°; RAAN 90°) com diferentes tempos de eclipse.

O estudo foi feito usando um programa MATLAB para analisar a energia consumida e o déficit de energia durante uma órbita e durante um dia.

Verificou-se que as órbitas com RAAN 0° e RAAN 53,5° podem completar a missão sem alterações. Porém, a órbita com RAAN 90° tem algum déficit acumulado após um dia que leva a insuficiência energética, a qual só é possível superá-la com algumas mudanças no algoritmo ou nos componentes usados.

Palavras-chave

CubeSat, nanosatélites, subsistema de gerenciamento de energia, raios cósmicos, órbita terrestre baixa, algoritmo, MATLAB.

Table of Contents

Chapter 1

1. Introduction	1
1.1. The project “ALSAT#1”	1
1.2. Methodology	3
1.3. Project Team	4
1.4. Cosmic rays	5
1.5. Small satellites and CubeSat	7
1.6. Previous work, project resume	9
1.7. Electrical power systems	14

Chapter 2

2. CubeSat components	15
2.1. Chosen components description	18

Chapter 3

3. CubeSat analyses	31
3.1. Power consumption diagram of the CubeSat sub-systems	31
3.2. Payload and communication Algorithm	33
3.3. MATLAB	35
3.3.1. Orbit RAAN 0°	35
3.3.2. Orbit RAAN 53.5°	37
3.3.3. Orbit RAAN 90°	39
3.3.4. Comparison among orbit RAANs	42
4. Conclusion	43
5. REFERENCES	44

List of Figures

Figure 1.1. ArduSiPM[2]	1
Figure 1.2. ADAA participants [1]	5
Figure 1.3. Cosmic rays spectrum [5].....	6
Figure 1.4. Secular variation of the semimajor axis for h = 500:800. First 180 days after January the 1st. [1]	10
Figure 1.5. Long-term periodical variation of the inclination for h=500:800 and RAAN0 = 0, $\pi/2$. First 180 days after January the 1st. [1].....	11
Figure 1.6. External temperature after January the 1st 2019. [1]	12
Figure 1.7. Internal temperature after January the 1st 2019. [1].....	12
Figure 2.1. Power output: mission duration relationship between energy source and appropriate operational scenario [15].....	15
Figure 2.2. EPS I power model [21]	19
Figure 2.3. UHF Transceiver Type II [23].....	21
Figure 2.4. Onboard Computer [25].....	23
Figure 2.5. UHF Antenna [29].....	26
Figure 2.6. 1U Solar Panel [30]	28
Figure 3.1. Power consumption diagram of the CubeSat sub-systems	31
Figure 3.2. Payload and communication Algorithm.....	33
Figure 3.3. algorithm exemplification for payload turn on or off	34
Figure 3.4. Orbit with Maximum eclipse time and without transmission time.....	36
Figure 3.5. Orbit with maximum eclipse time and maximum transmission time.	36
Figure 3.6. One day simulation with maximum eclipse time.	37
Figure 3.7. Orbit with Maximum eclipse time without transmission time.	38
Figure 3.8. Orbit with maximum eclipse time and maximum transmission time.	38
Figure 3.9. One day simulation with maximum eclipse time with time laps one minute.	39
Figure 3.10. Orbit with Maximum eclipse time without transmission time.	40
Figure 3.11. Orbit with maximum eclipse time and maximum transmission time.	40
Figure 3.12. One day simulation with maximum eclipse time with time laps one minute.	41
Figure 3.13. One day simulation with maximum eclipse time with time laps one minute, turning off payload in the communication zone.	41
Figure 3.14. One day simulation with maximum eclipse time with time laps one minute, with alternative OBC.....	42

List of Tables

Table 1.1. Relationship between the satellite class with the mass and cost. Source: [8]	8
Table 1.2. secular altitude variation [1]	11
Table 1.3. Eclipse Time [1]	11
Table 1.4. visibility times for one day $\epsilon=0^\circ$ [1].....	13
Table 1.5. Visibility times for one day $\epsilon=5^\circ$ [1]	13
Table 2.1. solar cell efficiency [16]	16
Table 2.2. Power Management and Distribution Systems [16]	16
Table 2.3. Battery Energy Density [16].....	17
Table 2.4. Electrical characteristics	20
Table 2.5. Electrical characteristics	22
Table 2.6. Electrical characteristics [25]	24
Table 2.7. Electrical characteristics	27
Table 2.8. Electrical characteristics	29
Table 2.9. Radiation degradation (remaining factor) [31].....	29
Table 3.1. Summary of the different orbit RAAN characteristics analyses	42

List of Acronyms

UBI	Universidade da Beira Interior
ADAA	associazione per la Divulgazione Astronomica e Astronautica
SiPM	Silicon PhotoMultipliers
LHC	Large Hadron Collider
CERN	European Organization for Nuclear Research
LEO	low earth orbit
OBC	On Board Computer
MIPS	Million instructions per second
QBT	Quantum Bit Technology
ESA	European Space Agency
ENAC	Italian Civil Aviation Authority (Ente Nazionale per l'Aviazione Civile)
GPS	Global Positioning System
RAAN	Right ascension of the ascending node
NASA	National Aeronautics and Space Administration
IGY	International Geophysical year
ICBMs	intercontinental ballistic missiles
VLSI	Very-Large Scale Integration
SSDL	Space Systems Development Laboratory
USA	United States of America
UHF	Ultra High Frequency
EPS	Electrical Power Subsystem
PMAD	Power Management and Distribution
TRL	Technology Readiness Levels
PCB	printed circuit board
RAM	Random-access memory
I ² C	Inter-Integrated Circuit
UFL	user function library
RF	radio frequency
MCX	micro coaxial connector
SPI	Serial Peripheral Interface
GEO	geosynchronous equatorial orbit
PCB	Printed Circuit Board

Chapter 1

1. Introduction

1.1. The project “ALSAT#1”

ADAA (associazione per la Divulgazione Astronomica e Astronautica) has the objective of creating a Satellite Development Centre, which intends to combine students and companies to produce a series of satellites with scientific purpose that are suggested and developed by students. [1]

For that objective, ADAA wish to involve students and institutes, using fewer money, to interact and communicate easily with a satellite, sheering the CubeSat mission philosophy.

In this way, ADAA is developing its first satellite called “ALSAT#1”. This satellite is envisaged to have an ArduSiPM as main payload when placed in orbit, this device allows to monitor the cosmic radiation using a Silicon PhotoMultipliers (SiPM) coupled to a sparkling crystal. This is an extremely sensitive light detector that can detect a single photon. When particles are detected, it becomes a nuclear radiation detector, in other words, a cosmic particles detector. Developed by INFN (Istituto Nazionale di Fisica Nucleare), Rome, with "Arduino DUE" card, ArduSiPM uses a Hardware / Software board that has as its processor a SAM3XE microcontroller from Microchip Technology, with ARM® Cortex™ -M3 core, and a custom board that contains electronics that can monitor, set and capture sensor signals (Fig. 1.1.).



Figure 1.1. ArduSiPM[2]

The ALSAT#1 CubeSat incorporates a voltage-controlled power supply, a fast preamplifier, a programmable discriminator capable of generating the digital pulse, a peak sensor for

measuring signal height, a temperature monitoring system, and a timer. This device was used in particle beam monitoring in one of the experiments of the LHC (Large Hadron Collider) at CERN (European Organization for Nuclear Research) in Geneva. Thanks to its excellent dynamics and the detection capability of single photons, the SiPM can be coupled with a scintillator crystal to build an efficient, small and robust radiation detector able to be carried into space in order to allow the characterization of cosmic radiation in low orbit (LEO) and a real-time comparison between the signal analysed in orbit with that detected at Earth through a correct network of distributed sensors. [1]

From a technological point of view, in order to ensure a high level of reliability in the development of the Alsat#1 satellite, and remaining within a relatively low-cost budget, ADAA has decided that the ATmegaS128 Microchip has the requirements to be the OBC (On Board Computer), which has a 8-bit microcontroller in RISC AVR® architecture in radiation-tolerant technology. The ATmegaS128 achieves execution speed of 1MIPS per MHz. The device uses 0.35 µm CMOS technology and high-density non-volatile memory technology (AT35K4 process). The ATmegaS128 has been developed and produced according to the requirements of the international standards MIL-PRF-38535 and AEQA0239. The quality and reliability of the ATmega S128 have been verified during normal product qualification in accordance to MIL-PRF-38535 and MIL-STD883. As a secondary OBC it was proposed to use a 8-bit microcontroller, also developed in radiation tolerant technology, the ATmegaS64M1.

When considering other segments of the mission, it is important to point out that the launch will be provided by the ESA through a Vega launcher. At the same time, the Ground Station for the mission is planned to be set at Malpensa Airport (Milan).

Moreover, a precursor flight is planned to be organized in order to test some components of the CubeSat such as payload, electronics and communication system. The required elements for this test are the following:

- Space balloon (2.5 Kg and $h_{max} > 40$ Km)
- Nylon rope
- Parachute
- Helium bottle ($V = 10$ m³)
- Notam ENAC (Authorization for the launch)
- Video camera 360°
- Video camera (redundancy)
- GPS tracker
- Thermal control system
- Radar reflector

1.2. Methodology

To complete the proposes designated to the Polytechnic of Milan for the ALSAT#1 mission, considering the orbit parameters already calculated in a previous study, an analysis in the power management subsystem of the CubeSat was done.

The previous study is focused in the analyse of many orbits between 500 km and 800 km, and the orbit selected is a sun-synchronous circular orbit at altitude 561 km; RAAN (Right ascension of the ascending node) 53.5°; Inclination 97.68°.

The Max. eclipsed time is an important factor for the sizing of the battery and the power available for the CubeSat, which is calculated to be 23.3 min. Another important factor is the transmission time, because in this period the satellite is consuming the maximum amount of energy. This is calculated to be 40 min of transmission time if data transfer is done during both day and night passes, otherwise it is only half of the time. It is also defined that the payload have a power consumption of 1 W.

According to this data, it was done a research for 1U CubeSat components that can allow the mission to be performed, this way we have an initial base to make the power consumption analysis.

For a better understanding of the energy dependence from the different components it is necessary to make a diagram which shows the power consumption of each one when they are on or off.

To analyse the power consumption during the mission, it was used a MATLAB program. First, it is made an algorithm for defining when the payload and the transmission subsystems are on or off, this way it is easier to explain how the program works and gives a base line to program the code.

The MATLAB analyses the different orbit conditions; for a single orbit the time passes in seconds and is done for:

an orbit with max. eclipse and with max. transmission

an orbit without eclipse and with max. transmission

an orbit with max. eclipse and without transmission

an orbit without eclipse and without transmission

It is also performed an analysis for a full day in the most critical period, that is when the satellite is performing the orbits with the max. eclipse time. To not have much programming time and overload MATLAB the time passes in minutes.

1.3. Project Team

The project is coordinated by a professional in the sector, Eng. Luca DEROSA, CEO of iMEX.A, with the participation of the following companies and universities [1]:

- University of Applied Sciences and Arts of Italian Switzerland- SUPSI (Manno - Lugano, Switzerland). With the contributions of Prof. Angelo CONSOLI (SAPHYRION) and Prof. Paolo CEPPI (SPACELAB), SUPSI joins ADAA in satellite design. Their expertise contributes for the study of thermal control, ground communications and on-board antenna design and related radio frequency circuitry.
- Milan Polytechnic University (Milan) - Department of Aerospace Sciences and Technologies. Prof. Franco BERNELLI, gives the structure to make the antenna for receiving the signal from the satellite on the ground, providing the team with an active support through some students for the development of the Mission Design, for the definition of the characteristics of the electric power generation and management system and for the attitude control.
- Microchip Technology (Legnano) - Aerospace Business Unit (formerly Atmel). It comprises the opportunity to bring on board three newly built microcontrollers in "radiation tolerant" space technology.
- INFN (Rome). Thanks to the support of Prof. Valerio BOCCI it has been possible to develop the payload in order to characterize cosmic radiations in low orbit due to energetic particles coming from the Sun that can damage the satellites in orbit and the earth, due to the highly energetic impacts with on-board electronic systems. Even if our atmosphere and the magnetic field of the Earth protect us partially from these radiations, we still need to monitor the big storms coming from our star. The CubeSat can help us by giving warnings and teaching us how to adapt our electronics to be more resistant, all due to the fact that the CubeSat is a great way to quickly perform experiments in space.
- iMEX.A (Turin). Engineering company specialized in aeronautics and space, works with ADAA for the structural design of the satellite, which is done with the innovative technology Additive Manufacturing.
- QBT (Quantum Bit Technology) (Chiasso): A leading company in the field of science and technology applied to the ICT sector. QBT takes care of defining the characteristics necessary for transporting and integrating our CubeSat into the launcher that will take it to the Space and also coordinates all the operations to be carried out during the mission in orbit, including activities with schools.
- LeafSpace (Lomazzo). Spin-off of the Politecnico di Milano, a company involved in making aerospace projects and interested in a close collaboration for the construction

and management of the Ground Station. LeafSpace is interested in helping ADAA to design an innovative satellite communication system to be implemented on board the ALSat#1 communication card.

- SpinElectronics (Turin). The Ing. Marco BRUNO, one of the leading national experts in satellite telecommunications, has become available for the operational choices in the field of communication between the satellite and the various ground stations and for the management of the payload activity (particle detector).
- BeamIT (Parma). The Italian company leader in the world for the creation of products through 3D printers with innovative materials. Thanks to the active support of Ing. Maurizio ROMEO, BeamIT takes care of the construction of the metal structure of the satellite.

The logos of the participants in the project are presented in Figure 1.2.



Figure 1.2. ADAA participants [1]

1.4. Cosmic rays

Cosmic rays are energetic, subatomic particles that arrive from outside the Earth's atmosphere. [3]

At the start of the 1900's, it was discovered that certain elements were unstable, being transformed into other elements, and in that process, emitting something that appeared to be particles, the process was called "radioactive decay". [3]

Also was noticed that an instrument called "electroscope" could measure the radioactive materials by discharging in their presence. However, electroscopes were slowly being discharged even in the absence of radioactive matter, and leakage couldn't be the cause, so there must be a background radiation. [3]

To study the source of this background radiation, in 1912, the physicist Victor Hess flew a high-altitude balloon. The objective was to understand if Earth was the source of that radiation. At the beginning, the radiation levels dropped a bit but then, started to increase with height. This result led him to conclude that there was radiation entering the Earth atmosphere from outer space. He gave to this phenomenon the name “cosmic radiation” which later evolved to “cosmic rays”. [4]

The lowest energy cosmic rays are produced by ordinary stars like the Sun. For example, when a solar flare occurs a lot of particles are ejected from the Sun, these particles interact with the Earth magnetic field and are attracted to the magnetic poles, where they excite the air in the ionosphere causing it to glow. This phenomenon is called Aurora. [3]

Cosmic rays generally collide with particles in the earth atmosphere inside the ionosphere causing the phenomenon called air shower. The air shower is like cascade of particles colliding until reaching the surface. We can perceive these events in the surface by detecting the muons that are sequent particles formed in the air shower.

The cosmic ray spectrum is presented in Figure 1.3.

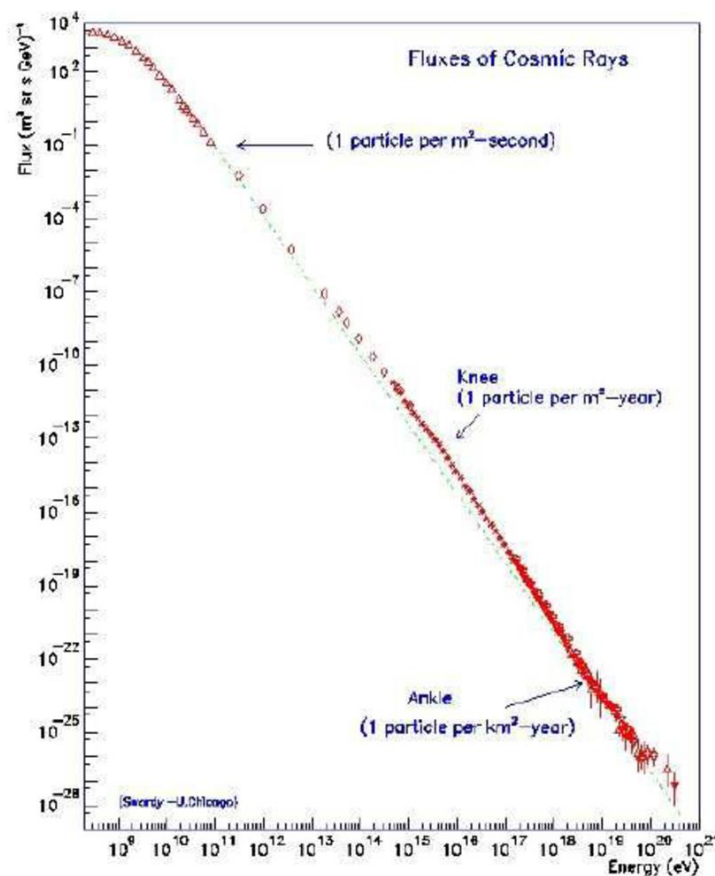


Figure 1.3. Cosmic rays spectrum [5]

Cosmic rays reach Earth with a variety of energies, the lowest energetic cosmic radiation is the most common and the majority are deflected or absorbed by our magnetic field and atmosphere. [3]

As the energy of the cosmic rays increases, the rate of particles decreases drastically and the path experience less deflection on the magnetic field and penetrate deeper into the atmosphere. Particles with intermediate energy levels, that are in the “Knee” of the cosmic radiation spectrum, are the “Very High Energy” cosmic rays and they have a frequency of appearance around one per square meter per year. The highest energy cosmic rays, in the region called “Ankle”, are the “Ultra High Energy” cosmic rays and have a rate of fall events around one per square kilometre per century. [3]

The source from where came the high energy cosmic rays is difficult to know due to the influence that magnetic fields cause to their passage but is supposed that they come from outside the solar system in energetic structures where strong shocks are expected to be found. Still, it is difficult to explain the existence of Ultra High Energy cosmic rays, because supernovae are simply not large enough to maintain acceleration for that particles. So, scientists suspect that other large-structures such as active galactic nuclei or colliding galaxies might be the responsible, nevertheless the source is still unknown. [3]

Scientists are trying to trace back cosmic rays origin by looking at their composition. The results from NASA show very common elements in the universe. Around 90 percent of cosmic rays are single protons and 9 percent are helium nuclei's (alpha particles). The remaining 1 percent are all the other elements, and the focus is to find rare elements and make correlations between different types of cosmic rays. Also, cosmic rays can be recorded by looking at radioactive nuclei's that decrease over time by measuring the half-life of each nuclei. [6]

Furthermore, the understanding of the space radiation is important for understanding the damage that could be caused from it to humans and machines in space missions.

1.5. Small satellites and CubeSat

The three first satellites: Sputnik-1, Explorer-1 and Vanguard-1, were the first's to be launched into low Earth orbit during the International Geophysical year (IGY) of 1957-1958 and started the space age. In that years, the United States and the Soviet Union were engaged in a “Cold War”. Both were developing nuclear weapons of mass destruction and intercontinental ballistic missiles (ICBMs) capable to strike the other. [7]

The first satellites were small, Sputnik-1 had 83.6kg mass, Explorer-1 had 13.9kg mass and Vanguard-1 had 1.47kg mass, this especially because the launchers limitation. [7] However, the need for more advanced and capable satellites, led to a natural growth in the satellite mass.

This trend was first limited by the available launcher’s capability and later by the finance and technological infrastructure, since not all nations were capable to spend so much money, being the space limited only to enormous military and economic nations. [8]

In the seventies, advances in Very-Large Scale Integration (VLSI) gave the chance to put sophisticated functions into very small volumes, with less mass and reducing the energy demand. This opened the door for the modern small satellites reducing dramatically the cost for satellite missions. [8]

In 1961, OSCAR-1, an amateur microsatellite radio transmitter box, has been built by enthusiasts from USA, USSR, Germany, Australia and Japan. This was the start of low-cost smaller satellites, despite, the last OSCAR-8 still without computer on board. [8]

Only in the eighties of las century started to be used small sophisticated satellites, with the launch of a microsatellite having an on-board computer, in 1981. This was the UoSAR-1 (UoSAT-OSCAR-9) and its success led directly to a second spacecraft UoSAT-2 (UoSAR-OSCAR-11). [8]

The UoSAR-1 operated for eight years until re-entering in the earth atmosphere and the UoSAT-2 remained operational for twenty years, despite having a planned three years mission life time. These two spacecrafts established the modern concept of a microsatellite. [8]

The table 1.1. shows the relationship between the satellite class with the mass and cost.

Table 1.1. Relationship between the satellite class with the mass and cost. Source: [8]

Class	Mass(kg)	Cost (million £)
Conventional large satellite	> 1000	> 100
Conventional small satellite	500 - 1000	25 - 100
Minisatellite	100 - 500	7 - 25
Microsatellite	10 - 100	1 - 7
Nanosatellite	1 - 10	0.1 - 1
Picosatellite	< 1	<0 .1

Not always a small, low cost satellite results in a low-cost mission. There are three main aspects that can influence the mission cost, and each element needs to be appropriately apportioned. The aspects and typical values proportions are: satellite cost = 70%; launch cost = 20%; orbital operations costs over lifetime = 10%. [8]

Therefore, to achieve low cost missions it is needed to apply a certain design philosophy to the entire mission. Following that philosophy, we have the CubeSats that are a small standardized satellite. This standardization allows the companies to mass produce components and reduce the cost. Also, the standard shape and size help to reduce cost associated with transporting and deploying them to space. CubeSats have many sizes, which are based on a standard CubeSat unit “1U”, that corresponds to a 10 cm cube with mass of approximately 1 to 1.33 kg. There

are other larger versions that become popular and use the same base unit, such as 1.5U, 2U, 3U and 6U, but different configurations can be done. [9]

This concept was first proposed by Professor Robert Twiggs at Stanford University's Space Systems Development Laboratory in 1998. The first CubeSat project began in 1999 from a collaboration between California Polytechnic State University (Cal Poly) and the Stanford University's Space Systems Development Laboratory (SSDL). [10]

Since the first CubeSat was launched, the number of CubeSats launched per year has increased and now, in total, more than a thousand of CubeSats were launched and the predictions are to continue to increase. [11]

In general, more than half of the CubeSats are from the USA and more than one quarter from Europe, being these two the major power in the CubeSat technology. Other countries like China, Japan, Canada, etc... have also some amount of less than 4%. It is estimated that 65 countries have nanosatellites. [11]

The organisation types that produce nanosatellites are mainly companies, which produce around half of the nanosatellites, and Universities that produce almost one third of the nanosatellites. Also, space agencies, Military agencies, non-profit organisations, institutes and schools have a contribution in the nanosatellites produced, of between 1-5% each one. [11]

The CubeSats have a planned life time of two to three years, but they can go up to 20 years of mission life time. The smallest CubeSat size used now is 0.25U and the biggest is 27U. [11]

In general, CubeSats are used in missions to low earth orbits due to their nature of being a more experimental satellite, but in 5th of May of 2018 two CubeSats were launched alongside NASA's InSight Mars lander mission. MarCO-A and MarCO-B were the first CubeSats to do an interplanetary mission. [12]

The CubeSats are mainly directed to experimental missions, but, in the future, other small satellites that follow the same logic of standardization and mass production to reduce the costs, can be used to revolutionise the telecommunications. Starlink is a program from the SpaceX to provide satellite internet access all over the world. It consists of a satellite constellation and is planned to have in total 12000 satellites deployed by the mid of the 2020's, with a possible later extension to 42000 satellites. The satellites will be placed in three different low earth orbits and from the prototypes, it is estimated that each satellite will have 227 kg. [13]

1.6. Previous work, project resume

The ALSAT#1 mission aims to study the cosmic rays in a LEO orbit in accordance with the duties assigned to the Polytechnic University of Milan. [1]

The objective of this thesis is to make a preliminary analysis of the ALSAT#1 mission.

The first studies were directed to analyse and select the possible orbit for the mission. Considering the requirements imposed by ADAA and the mission requirements, different Heliosynchronous orbits were analysed by parameterizing the altitude and the right ascension of the ascending node. In this regard, an heliosynchronous orbit from 500 km to 800 km will permit enough lifetime without important perturbations, removing the necessity of maintenance manoeuvres. Also, will provide the possibility of passing over the ground station always at the same local time, which is useful in order to fix certain times of linking and data transfer. Considering that, such ground station is to be situated in the Malpensa Airport (Milan).

One of the principal parameters evaluated was the perturbations caused by various sources like drag, Sun Moon gravity or j_2 , into the orbital parameters. These perturbations are important to analyse because they can make the satellite to lose orbital properties as heliosynchronism or pass in lower layers of the atmosphere. As we can see in the figures 4 and 5, the inclination was not significantly changed in the studied period. In the other hand, the altitude decay is mainly influenced by the altitude (Table 1.2.). When the orbits are above 700 km it remained almost at the same altitude. The lowest orbit (around 500 km) experiments a decrement of 14 km after 180 days.

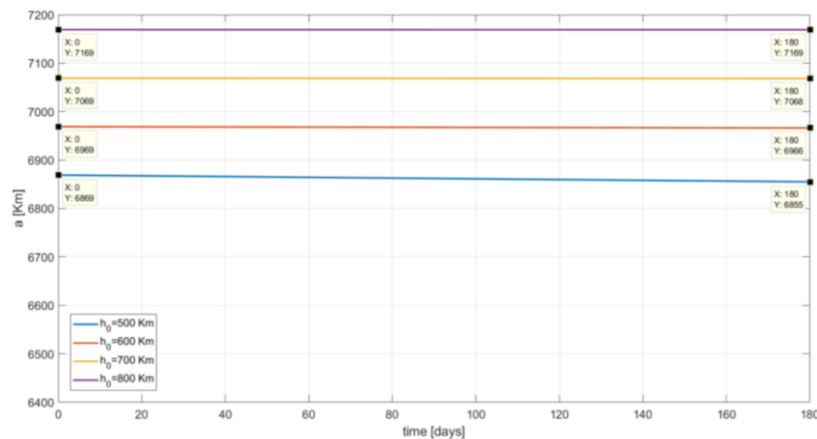


Figure 1.4. Secular variation of the semimajor axis for $h = 500:800$. First 180 days after January the 1st. [1]

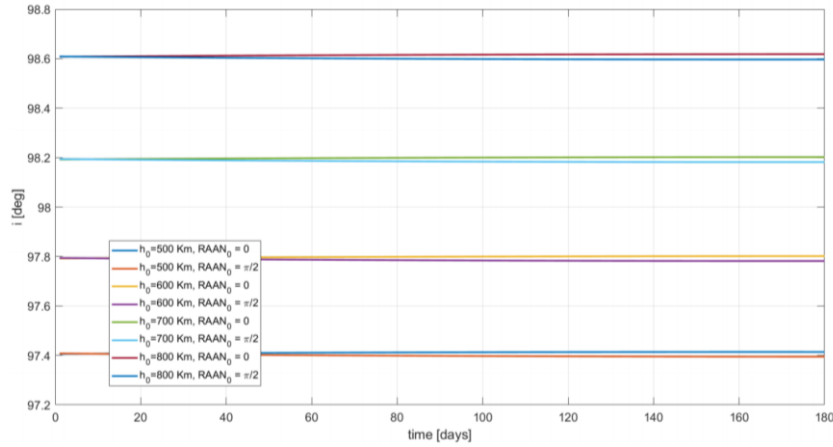


Figure 1.5. Long-term periodical variation of the inclination for $h=500:800$ and $RAAN_0 = 0, \pi/2$. First 180 days after January the 1st. [1]

Table 1.2. secular altitude variation [1]

Initial altitude h_0 [km]	Secular altitude decay [km] (after 180 days)
500	14
600	3
700	1
800	0

Other important thing to have in consideration in the orbit selected is the eclipses time (Table 3). This is very important for dimensioning many subsystems of the satellite like the Thermal and Power ones. In the results presented in table 1.3. we can see that the eclipse time is mainly reliant with the RAAN selected. More accurately, when selecting an orbit with descending node of 12:00 the eclipse time has an order of magnitude higher than that of the 18:00 descending node. Other thing observed is that for the 12:00 descending node the altitude of the orbit doesn't have a significant effect, otherwise, for the 18:00 descending node the highest orbit and the lowest orbit has a difference of almost 7 minutes.

Table 1.3. Eclipse Time [1]

ORBIT: h (Km) - Local Time of Descending Node (hh:mm:ss)	Maximum Eclipse Time (min)	Total Eclipse time over a year (h)
500-12:00:00	35.74	3312.0
600-12:00:00	35.48	3218.8
700-12:00:00	35.28	3133.9
800-12:00:00	35.14	3056.3
500-18:00:00	23.79	477.9
600-18:00:00	20.84	383.3
700-18:00:00	18.90	305.2
800-18:00:00	17.03	238.5

The following thing considered for the selection of the mission orbit are the temperatures that can face the system, once the mission components of the satellite must not overpass their structural and thermal limits. For that analyses It was used MATLAB with a simple two node model using RAAN and altitude of the orbit as main parameters. In the figures 1.6. and 1.7., it can be seen the internal and external temperatures for some orbits.

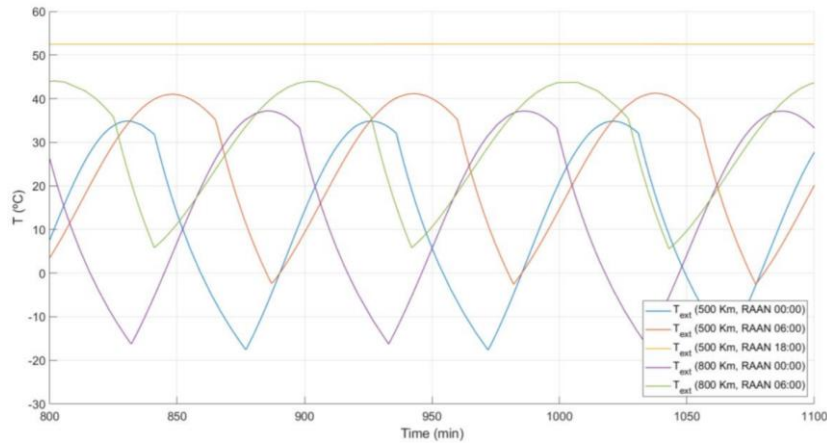


Figure 1.6. External temperature after January the 1st 2019. [1]

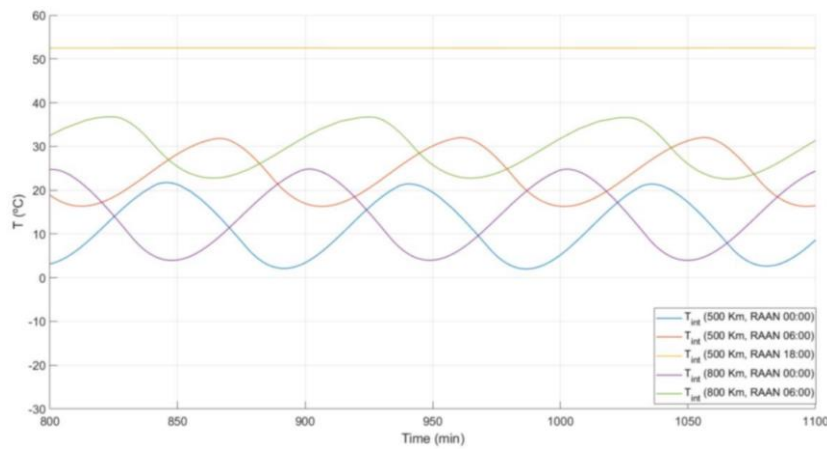


Figure 1.7. Internal temperature after January the 1st 2019. [1]

Also, a radiation analysis was carried out with the tool SPENVIS to rate the influence made by the different orbital elements on several types of particles and the total ionizing dose that may face the CubeSat.

Subsequently, analysing the results from the trade-off, the suggested orbit is a LEO sun-synchronous and Repeating Ground Track orbit. This allows the CubeSat to have a fixed position in respect to the sun and allows the CubeSat to pass over the same location at the same local time. The main orbital parameters of the orbit are the following:

- Altitude: 561 Km
- Inclination: 97.68°
- RAAN: 53.5°
- $e = 0$

For this orbit the perturbations in the inclination are insignificant for the time of the mission, while in 180 days the altitude decay will be 5 km.

The visibility time is also an important parameter (Tables 1.4. and 1.5.). The satellite is in the communication location when the satellite is in the visibility cone, that means when the satellite is in a cone with the centre on the ground station and a semi-angle of $90^\circ - \epsilon$, being ϵ (elevation) dependent on the obstacles around the ground station. For a ground station in the airport of Malpensa ϵ is less than five degrees angle. The total time in a day that the satellite is in the visibility cone with $\epsilon = 5^\circ$ is about 40 minutes. To have a good margin of security, considering that the information is only sent during the night or during the two accesses with higher elevation, the total time is reduced to 20 min. If considering a typical UHF (Ultra High Frequency) downlink Data Rate of 1kps the amount of information in a day is around 1.2 MB.

Table 1.4. visibility times for one day $\epsilon = 0^\circ$ [1]

Access	Start Time	Stop Time	Duration (min)
1	3:31:40	3:40:29	8.82
2	5:05:31	5:17:53	12.37
3	6:41:24	6:50:43	9.31
4	14:21:53	14:30:22	8.48
5	15:54:10	16:06:30	12.32
6	17:30:56	17:40:41	9.61

Table 1.5. Visibility times for one day $\epsilon = 5^\circ$ [1]

Access	Start Time	Stop Time	Duration (min)
1	3:34:00	3:38:00	4
2	5:07:00	5:17:00	10
3	6:43:00	6:49:00	6
4	14:24:00	14:28:00	4
5	15:55:00	16:05:00	10
6	17:33:00	17:39:00	6

1.7. Electrical power systems

The supply of electrical energy in space vehicles is an essential requirement for satellites payload. When power systems fail, it obligatorily results in the mission loss and is important to notice that many of the early satellite system failures are due to that loss. [8]

Usually, a spacecraft power system consists in three main elements: Primary and secondary energy sources, and a power control/distribution system. [8]

The primary energy source converts a fuel into electrical power. In the ALSAT#1 mission it are used solar arrays as the primary energy source and the fuel is the solar radiant energy. [8]

The secondary energy source is required to store energy and distribute electrical power to the satellite systems and payload for the time when the primary energy source is not available. For the ALSAT#1 mission the period where is necessary the secondary energy source is when the CubeSat is in eclipse time and the solar arrays are unable to produce electrical energy. [8]

The power control and distribution network, a more simply power management system, is required to deliver appropriate voltage-current levels to all spacecraft loads when required. [8]

An important aspect of the power management system is that it must be designed to operate with both energy sources, primary and secondary, whose characteristics are changing/degenerating with time. [8]

The starting point for any system is to define the electrical consumption of the satellite. In general, this is not constant during the mission or during a single orbit. So, for a mission analysis it must be considered the mission profile and consequently the power demand. [8]

The three critical issues that need to be considered are the orbit parameters, the nature of the mission (if is to make communication, extract data, or other) and the mission duration. [8]

The orbit selection has influence in the eclipse time and energy available; the nature of the mission has impact in the components that must be on or can be off during some periods and the energy consumption from components that are required for the mission; the mission duration has impact in the degradation of the components through time. [8]

Chapter 2

2. CubeSat components

There are many suppliers of CubeSat parts all over the world, in the nanosats.eu. [14] There is possible to see the companies that have identified themselves as CubeSat suppliers of Components, Testing Equipment/Components, Buses/Platforms, and Launch Services.

For the power system, the principal components that must be considered are the primary source of energy, the secondary energy source and the power management module that manage the distribution of energy.

The figure 2.1. below shows the different energy sources for space.

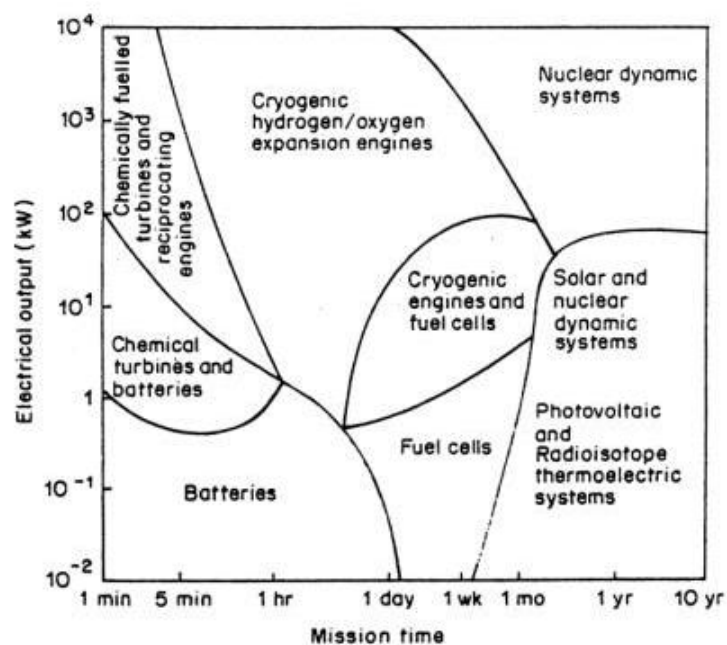


Figure 2.1. Power output: mission duration relationship between energy source and appropriate operational scenario [15]

Approximately 85% of the nanosatellites use solar cells as primary energy source and rechargeable batteries as secondary energy source, especially for their increased mission time and not carrying radioactive atoms. [16]

Based on the article, “State of the Art Small Spacecraft Technology” made by NASA, it is possible to see the available technology on the market until October 2018. [16]

Table 2.1. shows the available technology and their solar cell efficiency.

Table 2.1. solar cell efficiency [16]

Product	Manufacturer	Efficiency	Solar Cells Used	TRL Status
Solar Panel (0.5- 12U); Deployable Solar Panel (1U,3U)	AAC-Clyde	29.5%	SpectroLab XTJ	9
Solar Panel (0.5- 12U); Deployable Solar Panel (1U, 3U)	AAC-Clyde	29.6%	AzurSpace 3G30A	9
Solar Panel (5 x 5 cm, 1U, 3U, custom)	DHV	29.6%	AzureSpace 3G30C Advanced	9
Solar Panel	Endurosat	29.5%	CESI Solar cells CTJ30	9
NanoPower (CubeSat and custom)	GomSpace	29.6%	AzurSpace 3G30A	9
HAWK	MMA	29.5- 30.7%	SolAero XTJ & Prime	7
eHAWK	MMA	29.5- 30.7%	SolAero XTJ & Prime	9
COBRA	SolAero	29.5%	SolAero ZTJ	Unkn.
Space Solar Panel	SpectroLab	29.5%	SolAero XTJ	9
Space Solar Panel	SpectroLab	29.5%	SolAero XTJ Prime	6

Theoretically, the most efficient is the infinite-junctions with 86.6% in concentrated sunlight but the triple-junction solar cells have the best cost efficiency.

The general efficiency of the space solar cells is 29.5 %, there are higher, like the solar cell from MMA, but they have less area than other solar cells optimized for CubeSats, so the overall energy generated is less.

In the table 2.2. are shown some power modules with the power consumption of each one. There are also other great variety of EPS and PMAD available on the market not listed in this table.

Table 2.2. Power Management and Distribution Systems [16]

Product	Manufacturer	Technology Type	TRL Status	Power consumed (mW)
BCT CubeSat Electrical Power System	Blue Canyon Tech	EPS	*	*
CubeSat Kit EPS 1	Pumpkin, Inc.	EPS	9	*
CubeSat EPS Type I, II and I Plus	Endurosat	EPS	5-7	75
EPSL	NanoAvionics	EPS	9	150
LEO PCDU	Surrey	PMAD	9	*
Nanosatellite EPS	AAC-Clyde	EPS	8	*
NanoPower P31U	GomSpace	PMAD	*	160
P1U "Vasik"	Crystalspace	EPS	*	15
PCDU-2100, -2200, -2300	ÅAC Microtec	PMAD	*	*
Power Storage and Distribution	Tyvak	PMAD	*	*
3u cPCI Power Supply	SEAKR	EPS	9	*

*Need to contact seller for more information

EPS (Electrical Power Subsystem) typically has a main battery bus voltage of 8.2 V, but can distribute a regulated 5.0 V and 3.3 V to various subsystems. The EPS also protects the electronics and batteries from off-nominal current and voltage conditions.

PMAD (Power Management and Distribution) systems control the flow of power to spacecraft subsystems and instruments and are often custom designed by mission engineers for specific spacecraft power requirements. However, several manufacturers have begun to provide a variety of PMAD devices for inclusion in small spacecraft missions.

Because of the mass and volume requirements for small spacecraft, the batteries and cells are arranged according to specific energy, or energy per unit mass, and because of the extremely short life time of primary batteries the table 2.3. focus only in rechargeable batteries.

Table 2.3. Battery Energy Density [16]

Product	Manufacturer	Specific Energy (Whkg-1)	Solar Cells Used	TRL Status
40Whr CubeSat Battery	AAC-Clyde	119	Clyde Space LiPolymer	9
BAT-100	Berlin Space Technologies	58.1	Lithium-Ferrite (Li-Fe)	9
BP-930s	Canon	132	Four 18650 Li-ion cells	9
COTS 18650 Liion Battery	ABSL	90 - 243	Sony, MoliCell, LG, Sanyo, Samsung	8
NanoPower BPX	GomSpace	154	GomSpace NanoPower Li-ion	9
Rechargeable Space Battery (NPD-002271)	EaglePicher	153.5	EaglePicher Li-ion	7
Li-Po battery packs	Endurosat	123.8	LiPolymer	*

*integrated with the EPS (Energy Power system)

Battery life time is also an important aspect to consider, Lithium-based and nickel-based batteries deliver between 300 and 500 full discharge/charge cycles before the capacity drops below 80%. [17]

The current nine-point NASA scale Technology Readiness Levels (TRL) are the following [16]:

Level 1 - Basic principles observed and reported.

Level 2 - Technology concept and/or application formulated.

Level 3 - Analytical and experimental critical function and/or characteristic proof-of concept.

Level 4 - Component and/or breadboard validation in laboratory environment.

Level 5 - Component and/or breadboard validation in relevant environment.

Level 6 - System/subsystem model or prototype demonstration in a relevant environment (ground or space).

Level 7 - System prototype demonstration in a space environment.

Level 8 - Actual system completed and “flight qualified” through test and demonstration (ground or space).

Level 9 - Actual system “flight proven” through successful mission operations.

From the companies in tables 2.1., 2.2. and 2.3., only GomSpace, AAC-Clyde and Endurosat are the ones that provide all the necessary components to build a complete CubeSat, the others are specialised only in some components.

Despite a CubeSat being an experimental low-cost space mission, the rate of success is near the 60%. [18] To avoid problems with components that were never tested together, it was preferred to use all components from the same company, despite it could be used components from different companies, if necessary.

From the companies, the Endurosat [19], is the best option because it is specialised in 1U to 6U CubeSats and can provide technical support to build them. Also it has detailed information about the power consumption of the components, that is essential for the power analyses.

2.1. Chosen components description

For calculating the energy consumption of some components, it is necessary to use the following formula that relates the current consumption with the electric potential difference. [20]

$$I \times V = P$$

I is the current intensity in amperes, V the potential difference in volts and P the power in watts.

The components selected for the CubeSat are the following:

- 1x Power Module; EPS I (Fig. 2.2)

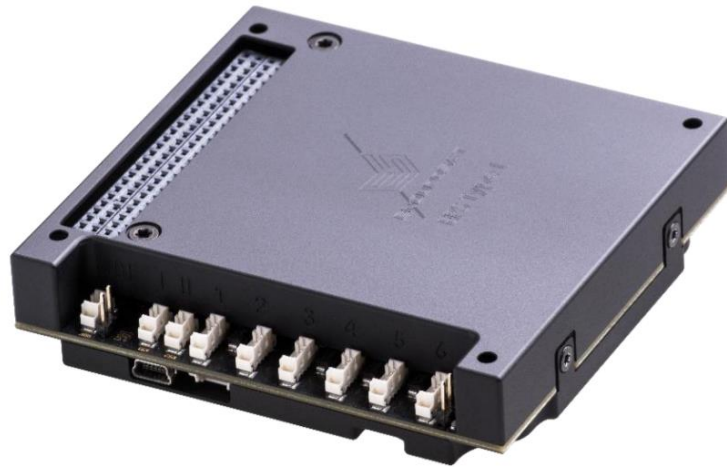


Figure 2.2. EPS I power model [21]

HIGHLIGHTED FEATURES [21]:

- Three solar panel channels (one for each CubeSat axis: x, y and z)
- Input voltage (per Solar Panel Channel): up to 5.5 V
- Input current (per Solar Panel Channel): up to 1.8 A
- Six connectors for the solar panels
- Integrated blocking diode for each solar panel connector
- Battery pack power: 10.4 Wh (20.8 Wh for two battery packs)
- Battery pack voltage: 3.7V nominal
- Very low power consumption in normal operation: 20mA @3.7V battery
- Stackable battery packs: up to 8A
- Output power buses: 3.3V, 5V, BCR (5Vmax) and 'battery raw'
- 3.3V and 5V latch-up protected outputs
- Interfaces: UART, I2C, USB (Virtual COM Port)
- Two deployment and one Remove Before Flight (RBF) switches can be connected
- Six general purpose outputs for shutdown/reset of external modules
- USB debug & battery charger
- Weight: EPS I = 208g (includes 1 battery pack)
- Weight: EPS I Plus = 292g (includes 2 battery packs)

The electrical characteristics of the EPS I are listed in table 2.4. [21].

Table 2.4. Electrical characteristics

Parameter	Unit	Condition	Min	Typ	Max
Battery Capacity					
Capacity	mAh	EPS with 1 battery pack	2640	2800	
	mAh	EPS with 2 battery packs	5280	5600	
	Wh	EPS with 1 battery pack		10.4	
	Wh	EPS with 2 battery packs		20.8	
Battery charger					
EOC voltage	V		4.08	4.1	4.12
Charge current	mA	Charge Mode 4	755	815	875
	mA	Charge Mode 3	540	580	620
	mA	Charge Mode 2	430	460	490
	mA	Charge Mode 1	215	230	245
Module Consumption					
Power consumption	mW	Normal Operation. LUP5V & LUP3V3 are OFF		75	
	mW	Low Voltage or High Temperature State. All Buses are OFF		43	
+ 5 V Bus					
Output voltage	V		4.88	5	5.15
Output current	mA	EPS with 1 battery pack			2000
	mA	EPS with 2 battery packs			4000
Operating frequency	kHz		500	535	560
Efficiency		$V_{batt} = 4$; $I_{5VBUS} = 2A$	82%	84%	86%

In normal operation the module consumes: 0.075W

The battery has four recharge modes, the typical power consumption can be calculated for each one:

$$\text{Charge mode 1: } 0.230A \times 4.1V = 0.943W$$

$$\text{Charge mode 2: } 0.460A \times 4.1V = 1.886W$$

$$\text{Charge mode 3: } 0.580A \times 4.1V = 2.38W$$

$$\text{Charge mode 4: } 0.815A \times 4.1V = 3.34W$$

The charge mode 4 needs more power than what is provided by the solar panels, so this one is excluded.

The typical efficiency of this battery is 84% using the +5V Bus.

The battery has an expected 500 cycles life of 2.196 Ah each. It was used the battery pack voltage of 3.7 volts to convert the energy consumed in 500 cycles to watts.

$$2.196Ah \times 3.7V \times 500 = 4062.6Wh$$

We can state that after using 4062.6Wh of battery energy, the battery has a 80% of its initial maximum energy capacity [17] [22].

- 1x UHF Transceiver Type II (Fig. 2.3.)



Figure 2.3. UHF Transceiver Type II [23]

HIGHLIGHTED FEATURES [23]:

- Frequency range (Tx/Rx): 400 to 403 MHz, and 430 to 440 MHz
- Modulation: OOK, GMSK, 2FSK, 4FSK and 4GFSK are optional, 2GFSK (by default)
- Automatic Frequency Correction
- Configurable AX.25 telemetry beacon broadcast
- Morse code
- Audio beacon
- Protocols: transparent, AX.25
- Maximum transmission power: 1 W; 30dBm (customizable up to 2 W; 33dBm)
- Power supply: 3.3 V (customizable to 5 V)
- Ultra-low power MCU with FRAM
- External FRAM
- Typical current consumption during receiving mode (idle mode) (Rx): 25mA @ 3.3V
- Frequency stability: +/- 2.5 ppm
- Data rate in the air: up to 19.2kbps (optional up to 100 kbps)
- Sensitivity: up to -121 dBm
- Communication interfaces: UART / I2C / USB (VCP) / RS485 (opt.) / CAN (opt.)
- Local and remote (in-flight) secured application firmware update
- Type: Half-duplex
- Weight: 94g

The planned UHF transceiver is estimated to have around 1kbps of data rate downlink. The UHF transceiver has 1.2 kbps minimum data rate in the transmitting mode, but with “bit slicing” it can be increased to 9.6kbps with a Packet Error Rate less than 1% when the signal-to-noise ratio is above 14 dB with similar amount of energy consumed. [23]

The UHF transceiver is totally encapsulated by an aluminum box that receives the heat from the power amplifier and protects the equipment from particle radiation.

There is also a second module that can be installed in the ground station to facilitate the uplink and downlink communication.

The electrical characteristics of the UHF Transceiver type II are listed in table 2.5. [23].

Table 2.5. Electrical characteristics

Parameter	Condition	Min	Typical value	Max
Supply Voltage [V]		3.2	3.3 ¹	5V Opt.
Current Consumption [mA]	Receive mode (Idle mode)	20	25 ²	30
	Transmit mode		413 ³	
	Continuous wave mode	700	780 ⁴	800
Operating temperature [°C]		-35		80

¹ This voltage directly supplies the internal power amplifier. Changes in the supply voltage will reflect in the output transmit power.

² Typical current consumption at 3.3Vdc power supply using only the UART and I²C interfaces (CAN and RS485 are turned off).

³ Typical current consumption depends on the ratio of transmit vs receive mode duration. For 50% Tx/50%, then the consumption would be as follows: 0.5*800 mA (Tx CW) + 0.5*25 mA (Rx)=413 mA @ 3.3 V.

⁴ Typical current consumption at 3.3Vdc and 435MHz working frequency

The typical consumption that the transceiver has in the transmit mode is:

$$0.413A \times 3.3V = 1.363W$$

And when the transceiver is in idle mode it is:

$$0.025A \times 3.3V = 0.0825W$$

- 1x Onboard Computer (Fig. 2.4.)

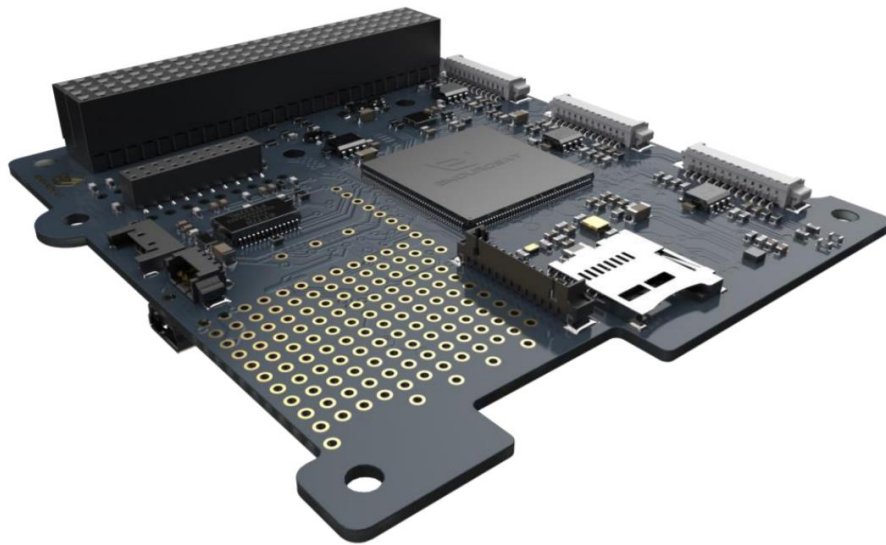


Figure 2.4. Onboard Computer [25]

For the onboard computer we have two options.

The first is the onboard computer that comes with all the other components and is full compatible with the CubeSat standards. It is based on ARM Cortex M4 with frequency rate up to about 180MHz, RAM 256KB, 2MB program memory size, 256Mbit Serial NOR Flash Memory and optional 64Mbit static RAM, the OBC has a total weight of 58g and 1.25 DMIPS/MHz [24].

This OBC comes with integrated double redundancy sensors (3-Axis accelerometers and compass), PWM drivers for magnetorquers and inputs for sun sensors, temperature sensors and gyroscope which allow the implementation of the attitude determination and control systems.

It is possible to connect additional PCB through connectors and mounting holes and to integrate easily additional sensors and chips such as atomic clocks, GPS receiver and so on.

The electrical characteristics of the Onboard Computer are listed in table 2.6. [25].

Table 2.6. Electrical characteristics [25]

Parameter	unit	Condition	Min	Typ	Max
Supply voltage	V		3	3.3	3.6
Supply current	mA	STM32F427@185Mhz		104	123
	mA	STM32F427@120Mhz		58	72
	mA	STM32F427@60Mhz		30	38
	mA	STM32F427@16Mhz		13	27
	µA	3-Axis Accelerometer - Normal Mode ¹	200		400
	µA	3-Axis Accelerometer - Low Power Mode ¹	8		12
	µA	3-Axis Accelerometer - Power Down Mode ¹	0.1		2
	µA	3-Axis Digital compass - Power Down Mode ²		1	
	µA	3-Axis Digital compass - Power Down Mode ² - Low Power Mode		40	
	µA	3-Axis Digital compass - Power Down Mode ² - High Resolution Mode		280	
	mA	Ext. 64M-bit Static RAM (Opt.), F = 18Mhz		45	55
	mA	Ext. 64M-bit Static RAM (Opt.), F = 1Mhz		8	48
	µA	Ext. 64M-bit Static RAM (Opt.), Stand-By Mode		4	15
	mA	Ext. 1 Gbit NOR Flash Memory Operational Mode @54Mhz (fast-read extended I/O)		6	6
	mA	Ext. 1 Gbit NOR Flash Memory Operational Mode @108Mhz (fast-read dual I/O)			18
	mA	Ext. 1 Gbit NOR Flash Memory Operational Mode @ 108Mhz (Operating current (fast-read extended I/O))			20
µA	Ext. 1 Gbit NOR Flash Memory Operational Mode Standby Mode			200	
Operating Temperature	°C		-30		85
Storage Temperature	°C			25	

¹ - Current consumption is for one 3-Axis Accelerometer. The OBC has two identical sensors on the same location, but on opposite sides of the PCB.

² - Current consumption is for one 3-Axis Digital Compass. The OBC has two identical sensors on the same location, but on opposite sides of the PCB.

Comparing with the OBC planned to be used for the mission the endurosat OBC had more capacity than needed even when used the minimum frequency (STM32F427 @16Mhz). The maximum consumption for this frequency can be calculated by multiplying the voltage with the current consumption $I \times U = P$.

The typical consumption of STM32F427 @16Mhz is: $0.013A \times 3,3V = 0.0429W$

The 3-axis accelerometer and the 3-axis compass in the max performance mode is: $(2.8 * 10^{-4} \times 2 + 4 * 10^{-4} \times 2)A \times 3.3V = 0.00497W$

Because the optional extra RAM will not be needed it is not necessary to make the calculations.

The Nor flash memory has a significant consumption only when reading the information, generally it is used to transmit stored information. [26]

The normal mode consumption of Nor flash memory is: $0.004A \times 3.6V = 0.0144W$

The standby mode consumption of Nor flash memory is: $2 * 10^{-4}A \times 3.6V = 0.00072W$

The overall endurosat OBC consumption is: $0.0144 + 0.00497 + 0.0429 = 0.0623W$

The backup OBC ATmegaS128, at max frequency 8MHz has a typical current consumption of 5mA [27] corresponding to: $0.005A \times 3.3V = 0.0165W$

And the Power-down mode has a current consumption of 10µA [27] corresponding to: $10^{-5}A \times 3.3V = 3.3 * 10^{-5}W$

The second OBC ATmegaS64M1 that will also operate with the ATmegaS128 has a typical current consumption at 8MHz of 3,8mA [28] corresponding to: $0.0038A \times 3.3V = 0.01254W$

And the Power-down mode has a current consumption of 9µA [28] corresponding to: $9 * 10^{-6}A \times 3.3V = 2.97 * 10^{-5}W$

Having the ATmegaS128 operating and the ATmegaS64M1 with power-down the total consumption is around 0.0168W, which corresponds to 73.0% less power consumption.

Having the ATmegaS64M1 operating and the ATmegaS128 with power-down the total consumption is around 0.01287W, which corresponds to 79.3% less power consumption.

- 1x UHF Antenna (Fig. 2.5.)

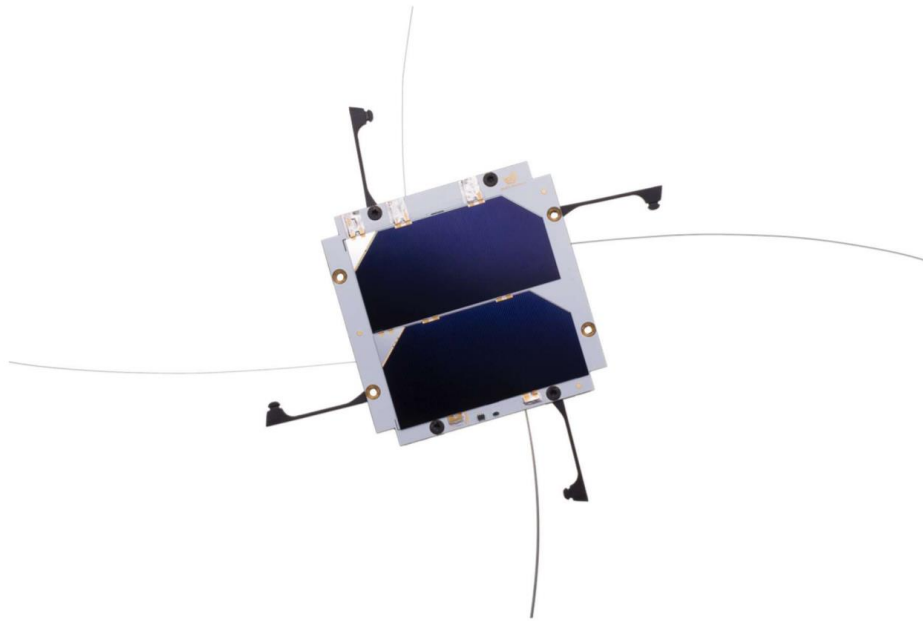


Figure 2.5. UHF Antenna [29]

HIGHLIGHTED FEATURES [29]

- UHF band for amateur satellite communications 435 - 438MHz
- Compatible with EnduroSat Solar panels
- Circularly polarized
- Weight: 85 g
- Gain > 0dBi
- Max RF output power 3.5W
- Burn wire mechanism with feedback for deployment
- Supply voltage: 5V
- I²C interface for monitoring and control
- Two redundant channels for direct deployment of the antenna rods with logical level
- Typical current consumption during antenna deployment: 250mA @5V
- Ultra-low current consumption in idle mode: 1mA @5V
- Rod deployment-controlled sequence
- Two algorithms for antenna deployment
- Test mode jumper for I²C verification and preventing for unwanted deployment of the antenna
- MCX Connector and secondary UFL connector inside the antenna for compatibility with different kind of satellite structures.

The antenna is designed to cover the amateur satellite band 435-438 MHz. It has a circular polarization and uses a dual redundant burn wire mechanism with double feedback for the deployment of the antenna rods. The antenna is controlled and monitored via I²C interface. It has an additional redundancy feature for direct control of the burning resistor chains via general purpose inputs.

The antenna is compatible and can come also with the solar panel.

The electrical characteristics of the UHF Antenna are listed in table 2.7. [29].

Table 2.7. Electrical characteristics

Parameter	Condition	Min	Typ	Max
Supply Voltage [V]		4.8	5	6
Current Consumption [mA]	Idle mode		0.5	2*
	Primary burning resistor		250	280
	Primary and Back-up burning resistor		500	560
	All primary burning resistors (pin 5 activated)		1000	1120
	All back-up burning resistors (pin 6 activated)		1000	1120
Burning resistors voltage activation [V]	Logical level threshold for activation of all burning resistors (primary or back-up burning wire resistor chains - pin 1, 2	1.5	3.3	6

*Peak current consumption during I2C communication with 4.7 kOhm pull-up resistors

The antenna has at idle mode a consume of $0.001A \times 5V = 0.005W$

The max consumption in the deployment is estimated to be 3.5W, but this is only for few moments. It is necessary the use of the battery and the payload can be turned on after the deployment.

Because the amount of energy consumed by the deployment occurrence is for a short period, it is not considered, so the MATLAB program starts after the deployment when the CubeSat is fully operational.

- 6x 1U Solar Panel (one for each side) (Fig. 2.6.)

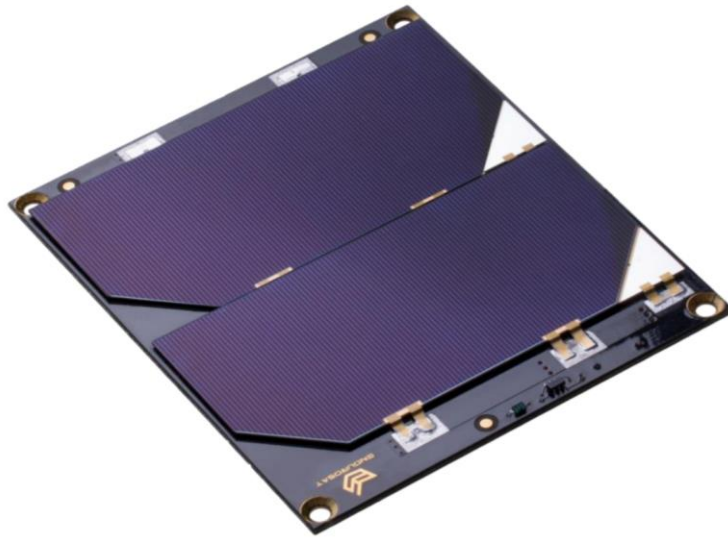


Figure 2.6. 1U Solar Panel [30]

Solar Panel Features and Characteristics [30]

- Two CESI Solar Cells CTJ30, space qualified triple junction (specs in the following paragraph)
- 60.30cm² effective cell area (2 solar cells)
- Temperature Sensor with SPI Interface (Accuracy: $\pm 1.5^{\circ}\text{C}$ from -25°C to 85°C (max), $\pm 2.0^{\circ}\text{C}$ from -55°C to 125°C (max))
- Up to 2.4 Watt in LEO
- Gold plated invar interconnectors
- Space-grade silicone adhesive with minimum outgassing behaviour
- Gyroscope
- Sun Sensor
- Multiple panels can be connected in series or parallel
- Two internal 70 μm copper layers
- Plated, countersink mounting holes with ground connection
- Connector for external magnetorquer
- Max Voltage: up to 4.66V (for 2 cells)
- Max Current: up to 517mA
- Thickness 2.2 mm ± 150 μm

Solar Cell Features and Characteristics [30]

- Efficiency up to 29.5%
- Triple Junction Solar Cells InGaP/GaAs/Ge
- Very low solar cell mass (81-89 mg/cm²)
- Thickness 155 $\mu\text{m} \pm 15 \mu\text{m}$
- Fully qualified under ESA Standard ECSS E ST20-08C for LEO and GEO
- Internal by-pass diode for optimized output power
- Size 30.15 cm²
- High radiation resistance
- Cover glass CMG (150 μm thick)
- Good mechanical strength

The electrical characteristics of the UHF Antenna are listed in table 13 and the radiation degradation in table 2.8. [30]

Table 2.8. Electrical characteristics

SOLAR CELL STRING					
parameter	Unit	Condition	Min	Typ	Max
Voltage	V	25°C			4.66
Current	mA	25°C			517
Power	mW	25°C			2400
Efficiency	%	25°C			29.5

Table 2.9. Radiation degradation (remaining factor) [31]

ELECTRON ENERGY	FLUENCE (e/cm ²)	I _{sc}	V _{oc}	P _M
1 MeV	1*10 ¹⁴	0.99	0.98	0.97
1 MeV	5*10 ¹⁴	0.96	0.95	0.91
1 MeV	1*10 ¹⁵	0.91	0.93	0.84

The solar panels tend to deteriorate with time due to the ionizing particles. This is generally measured with the equivalent of 1 MeV electron/cm² cumulated damage, in other words the total radiation dose is turned to the equivalent number of the damage caused by electrons with 1 MeV energy for each cm² of surface.

Based in a similar mission with almost identical orbit parameters, a 150 μm cover glass solar cell receives around 7*10¹³ (e/cm²) of total radiation dose in 3 years. [32]

The actual direct solar irradiance at the top of the atmosphere fluctuates by about 6.9% during a year (from 1.412 kW/m² in early January to 1.321 kW/m² in early July) due to the Earth's varying distance from the Sun. [33]

In this way, the minimum power available for a solar panel perpendicular to the sun is calculated as:

$$1321 \frac{W}{m^2} \times \frac{30.15 * 2}{100^2} m^2 \times 29.5\% \simeq 2.35 W$$

And after around four years mission the minimum power available for a solar panel perpendicular to the sun is estimated to be:

$$1321 \frac{W}{m^2} \times \frac{30.15 * 2}{100^2} m^2 \times 29.5\% \times 0.97 \simeq 2.28 W$$

Chapter 3

3. CubeSat analyses

3.1. Power consumption diagram of the CubeSat sub-systems

The diagram below summarises the power consumption and dependence of each component (Fig. 3.1.).

The solar panels are responsible to produce energy and send it to the power management to be distributed.

The power management subsystem is responsible for distributing the power received from the solar panels to the rest of the subsystems and it is also responsible for recharge and discharge the battery.

The onboard computer is responsible for processing the data received from the other subsystems and determine the activity of the telecommunications and the payload.

The antenna is dependent from the telecommunications. In deployment it has a maximum consume of 3.5W for a short period of time and in that period, it needs to use the battery.

The telecommunications are responsible for transmitting the data created by the payload. It operates only when the CubeSat is in the communication zone.

It is defined that the payload consumes a maximum of one watt.

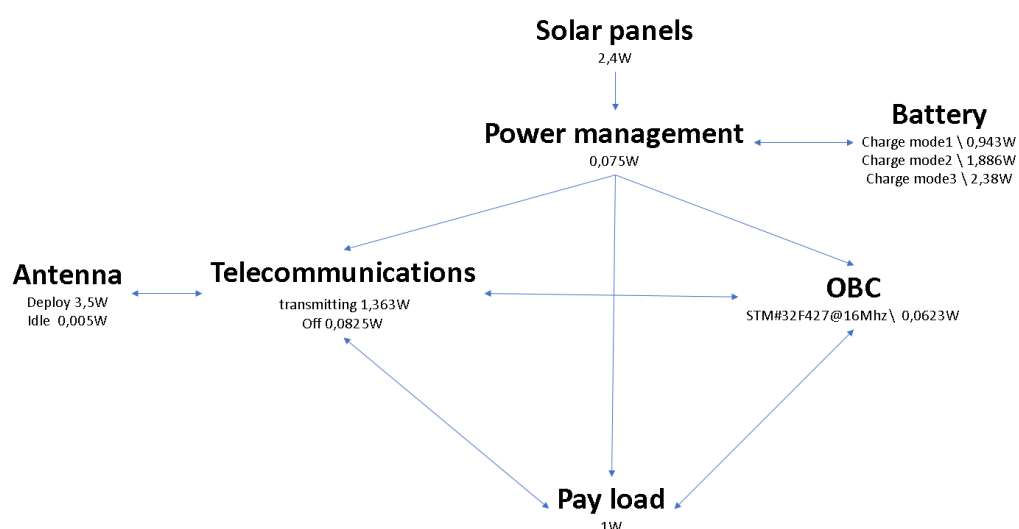


Figure 3.1. Power consumption diagram of the CubeSat sub-systems

The energy consumed in different situations is calculated as follow:

Energy consumed when payload is on and communication is off:

$$0.075W + 0.0623W + 0.005W + 1W + 0.0825W = 1.2248W$$

Energy consumed when payload is off and communication is on:

$$0.075W + 0.0623W + 0.005W + 1.363W = 1.5053W$$

Energy consumed when payload is on and communication is on*:

$$0.075W + 0.0623W + 0.005W + 1W + 1.363W = 2.5053W$$

Energy consumed when payload is on, communication is off and recharge mode1 is on:

$$0.075W + 0.0623W + 0.005W + 1W + 0.0825W + 0.943W = 2.1678W$$

Energy consumed when payload is off, communication is on and recharge mode1 is on*:

$$0.075W + 0.0623W + 0.005W + 1.363W + 0.943W = 2,4483W$$

Energy consumed when payload is off, communication is off and recharge mode2 is on:

$$0.075W + 0.0623W + 0.005W + 0.0825W + 1.886W = 2,1108W$$

*the energy demand is bigger that the given by the solar panels.

3.2. Payload and communication Algorithm

The algorithm below shows when the payload and the communications are going to be on or off (Fig. 3.2.).

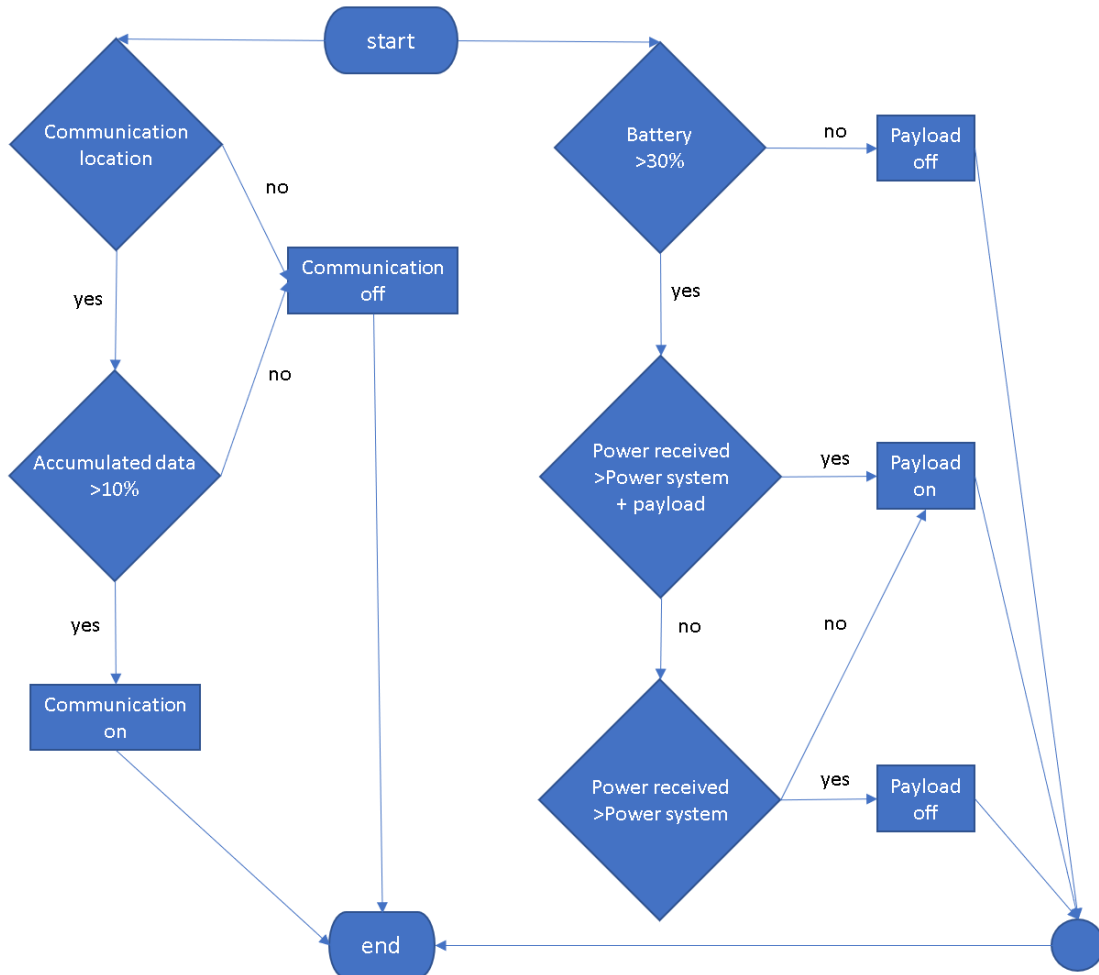


Figure 3.2. Payload and communication Algorithm

First, for the communication to be active it is necessary that the satellite is in the communication location, which is inside the visible cone; if it is outside it is in a standby mode. Other important thing is that the CubeSat needs to have data to be transmitted. Considering that the shortest period of transmission, according to the previous work, is 4 minutes in a total of 40 minutes, it is necessary to have at list 10% of the memory with data to be worthwhile to activate the communication.

Furthermore, to determine if the payload is on or off it is necessary to know if the battery is not at critical power levels. If the battery is not at critical power levels, the payload is off only when the power consumption of all the other components and the power consumption of the payload are more than the power received from the solar panels (when out of eclipse). In this

way, if the satellite is consuming more than what the solar panels can produce, the payload is turned off avoiding spending the battery life cycles.

To ensure that, first is checked if the power consumed from the systems plus the payload active is more than the power received, and subsequently, if the power received is higher than the power of the systems, in this way we know for sure that the battery is not already being used.

Figure 3.3. exemplifies the case.

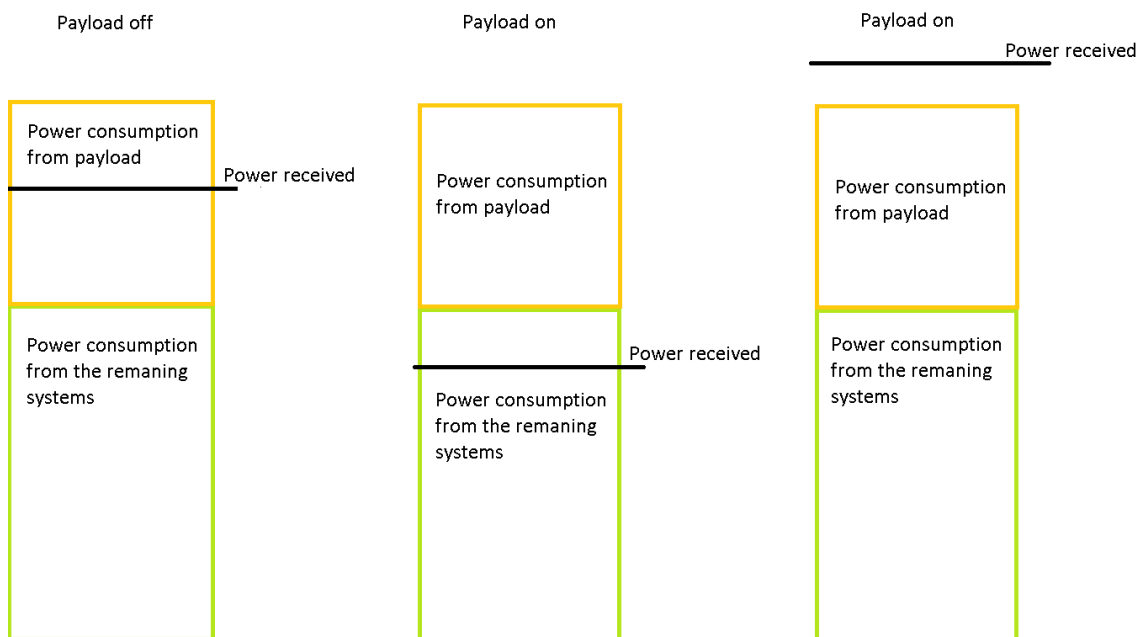
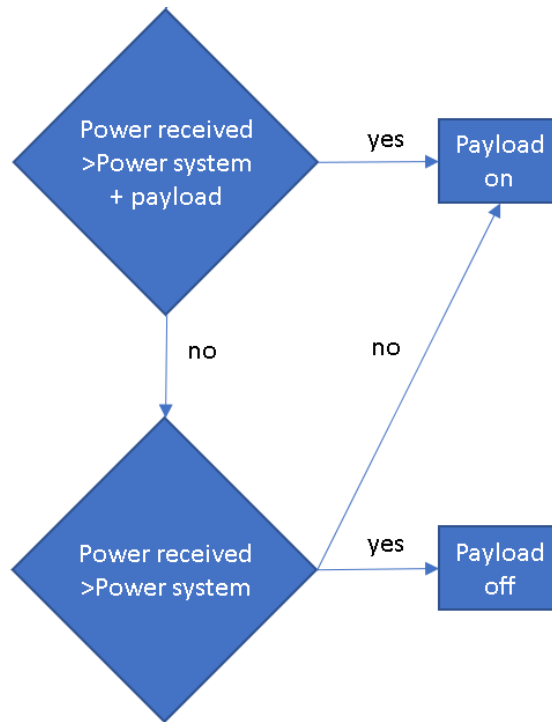


Figure 3.3. algorithm exemplification for payload turn on or off

3.3. MATLAB

It was created a programme in MATLAB following the logic of the algorithm, in order to simulate how the CubeSat performs.

Also, it was made a programme in MATLAB with cooperation with other student to simulate all the eclipse time that a satellite with specific orbit characteristics has in a year, which allows to calculate the battery used during that period.

The programme runs three different simulations:

- Maximum eclipse time and maximum transmission time, one orbit with time laps of one second.
- Maximum eclipse time without transmission time, one orbit with time laps of one second.
- One day simulation with maximum eclipse and time with time laps of one minute.

And three different orbit RAAN in order to test if the CubeSat is self-sustainable for different orbits. The simulations are made also for three different orbit RAAN's:

- RAAN=0°
- RAAN=53.5°
- RAAN=90°

The MATLAB programme shows 2 graphics, one with the power consumption and power received and the other with the energy deficit, both in order to time. The time of the eclipse is always rounded in excess to avoid having an optimistic simulation.

To optimize the battery life time, the batteries must work between 30% to 80% of the state-of-charge, this is the most effective bandwidth for lithium-based batteries and is usually called the sweet zone [17].

That means that the max energy deficit, considering the 0 Wh energy deficit at 80% of the battery capacity, are less than 5.2Wh in module.

3.3.1. Orbit RAAN 0°

The 0° RAAN orbit is the orbit with less eclipse time; the orbit with max eclipse time is less than 24 minutes.

Orbit with Maximum eclipse time and without transmission time; Orbit with maximum eclipse time and maximum transmission time

We can see in the graphics below (figs. 3.4. and 3.5.) that the energy deficit is fully recovered in a single orbit including when there is maximum transmission time.

The max energy deficit generated in an orbit is less than 0.8 Wh what means the battery can work in the battery sweet zone.

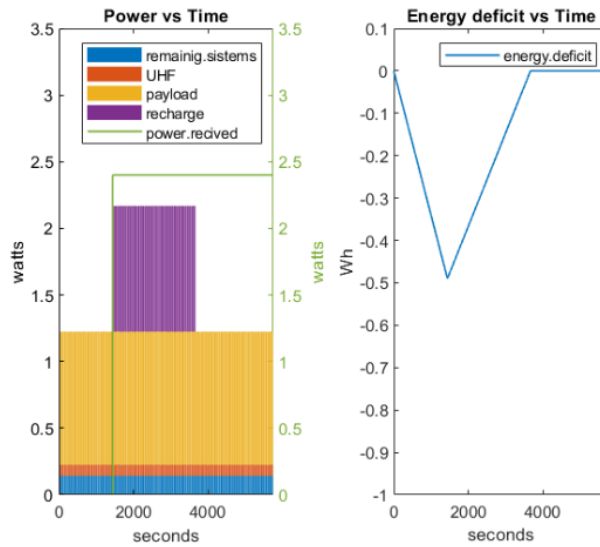


Figure 3.4. Orbit with Maximum eclipse time and without transmission time.

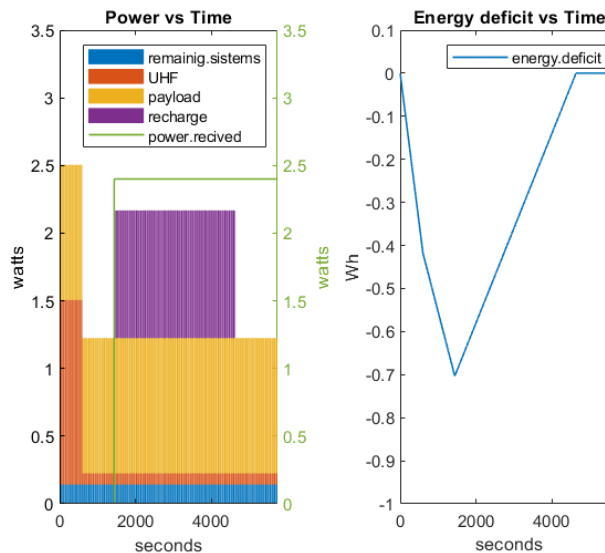


Figure 3.5. Orbit with maximum eclipse time and maximum transmission time.

One day simulation with maximum eclipse time

The graphic below (Fig. 3.6.) proves that the CubeSat has enough power during the max eclipse time orbits and the energy deficit can be fully recovered for all orbits during a day.

The overall battery used during a year is 596.5 Wh.

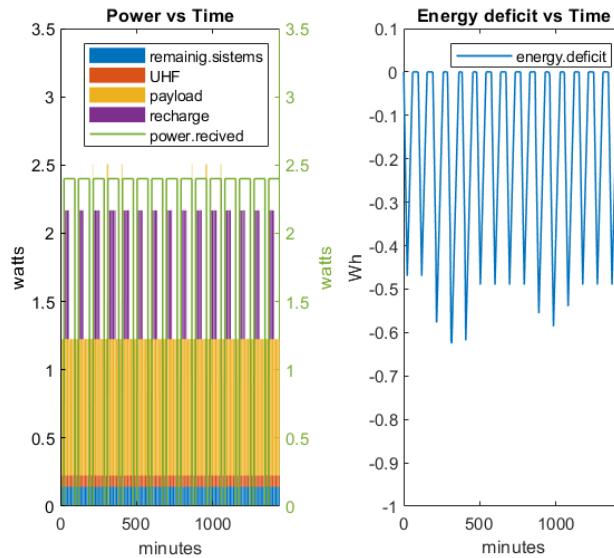


Figure 3.6. One day simulation with maximum eclipse time.

3.3.2. Orbit RAAN 53.5°

The 53.5° RAAN orbit is the orbit proposed for the CubeSat mission; during a year the orbit with maximum eclipse time is less than 31 minutes.

Orbit with Maximum eclipse time without transmission time; Orbit with maximum eclipse time and maximum transmission time

The graphics below (Figs. 3.7. and 3.8.) show that the CubeSat can fully recover the energy deficit in an orbit with max eclipse time and without transmission time, but an orbit with max transmission time it ends with a small amount of energy deficit.

The max energy deficit generated in an orbit is less than 0.9 Wh what means that the battery can work in the battery sweet zone.

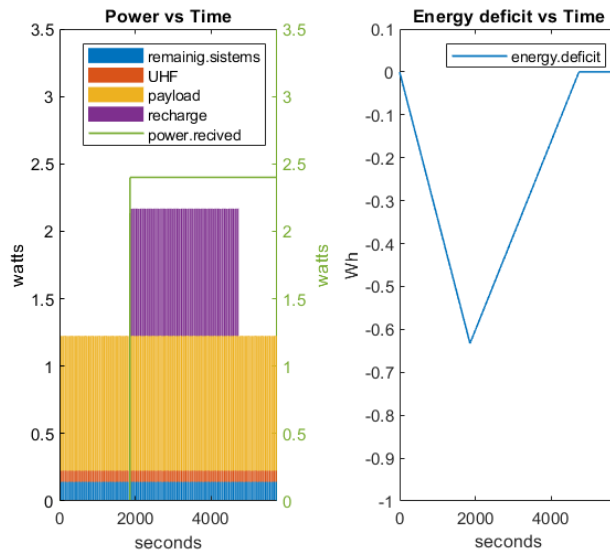


Figure 3.7. Orbit with Maximum eclipse time without transmission time.

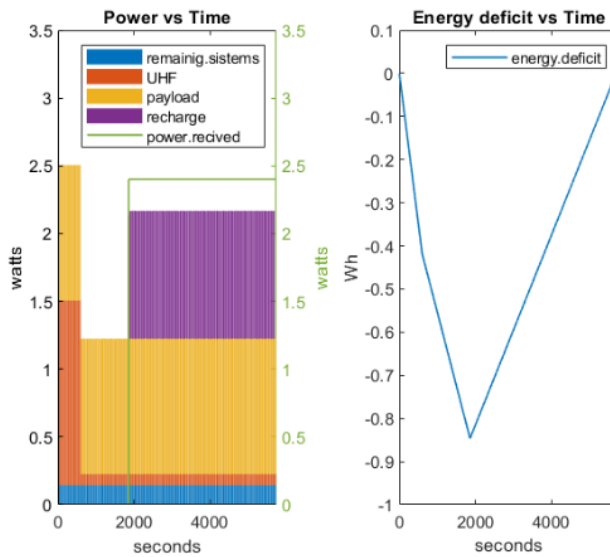


Figure 3.8. Orbit with maximum eclipse time and maximum transmission time.

One day simulation with maximum eclipse time with time laps one minute

The one-day simulation shows that, despite that small amount of energy deficit during the maximum eclipse and communication time, the CubeSat can fully recover without turning off the payload (Fig. 3.9.).

The overall battery used during a year is 3484 Wh.

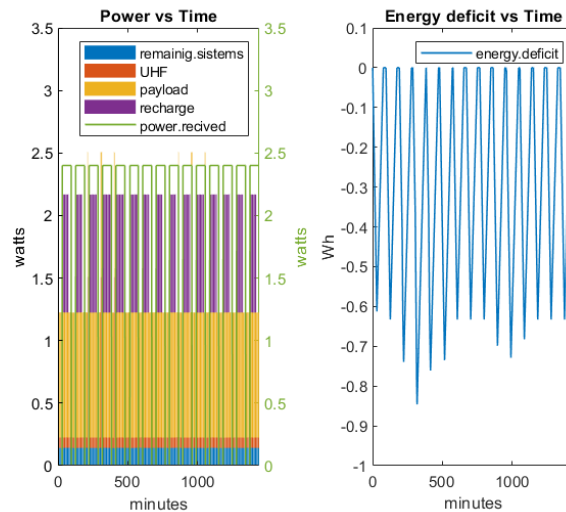


Figure 3.9. One day simulation with maximum eclipse time with time laps one minute.

3.3.3. Orbit RAAN 90°

This orbit is the orbit with larger eclipse time, it is approximately constant and less than 36 minutes. This orbit is of interest because if the CubeSat has enough power available it can perform in any other orbit.

Orbit with Maximum eclipse time without transmission time; Orbit with maximum eclipse time and maximum transmission time

In the graphics bellow (Figs. 3.10. and 3.11.) we can see that the energy deficit can be fully recovered in the orbit whit maximum eclipse time and without transmission time, but when there is transmission the energy deficit in the end of the orbit is -0.1597 Wh.

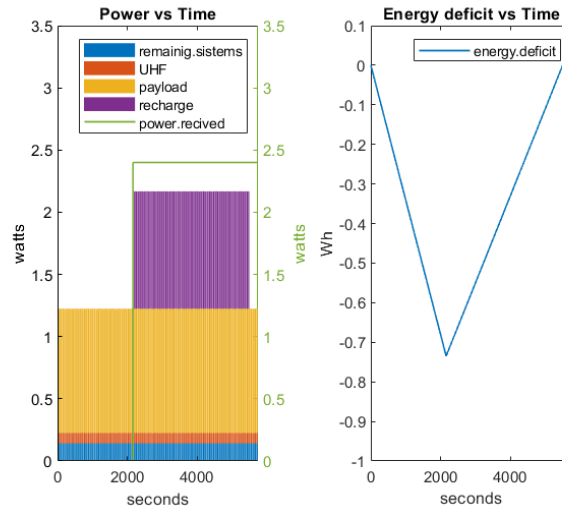


Figure 3.10. Orbit with Maximum eclipse time without transmission time.

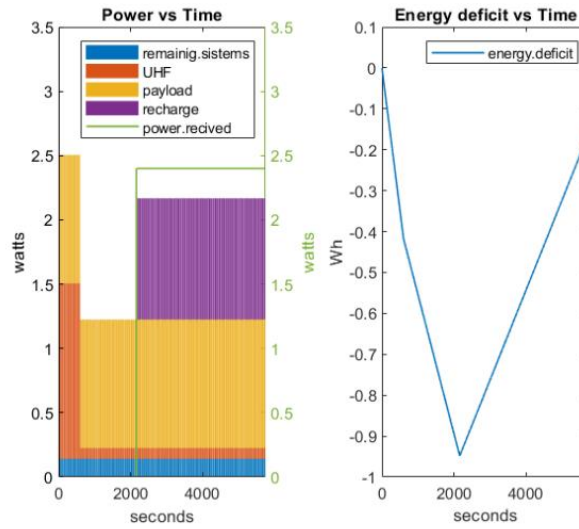


Figure 3.11. Orbit with maximum eclipse time and maximum transmission time.

One day simulation with maximum eclipse time with time laps one minute

In the one-day simulation it was calculated that since the start of the last communication and the beginning (12 hours period) of the next the CubeSat has an estimated -0.0607 Wh energy deficit (Fig. 3.12.).

The max energy deficit generated in an orbit is less than 1 Wh what means the battery can work in the battery sweet zone.

The overall battery used during a year is 4064 Wh.

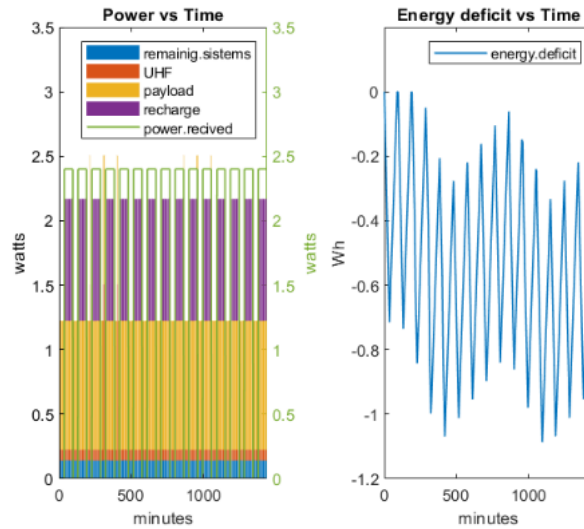


Figure 3.12. One day simulation with maximum eclipse time with time laps one minute.

This deficit would lead to a half battery energy consumption in 43 days. It can be easily avoided if used all the energy available left to recharge, but that requires change in the recharge mode. Also, with time, the solar panels experience degradation reducing the power available and the energy from the sun experiences some fluctuations depending on the distance we are from it, so some margin is necessary.

A Simpler solution is turning off the payload when the CubeSat is in the communication zone reducing the pick of energy consumption and avoiding to create a big energy deficit. The figure 3.13. shows it.

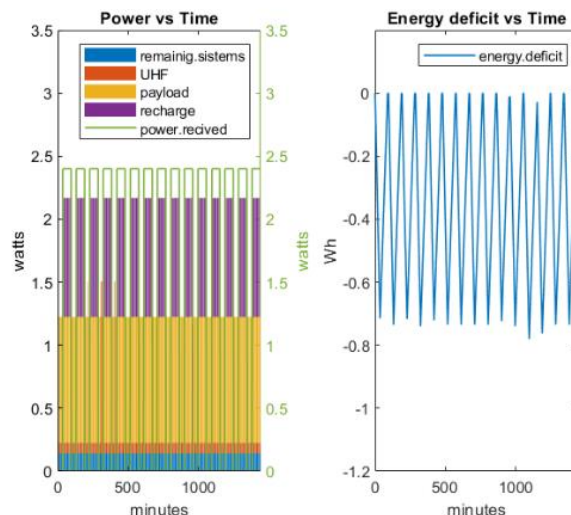


Figure 3.13. One day simulation with maximum eclipse time with time laps one minute, turning off payload in the communication zone.

Another solution is to change the OBC to the alternative one. Despite it are needed some adaptations and reconfiguration to work with the other components, the reduction in the power consumption allows the CubeSat to perform without changing the algorithm. The figure 3.14. shows it.

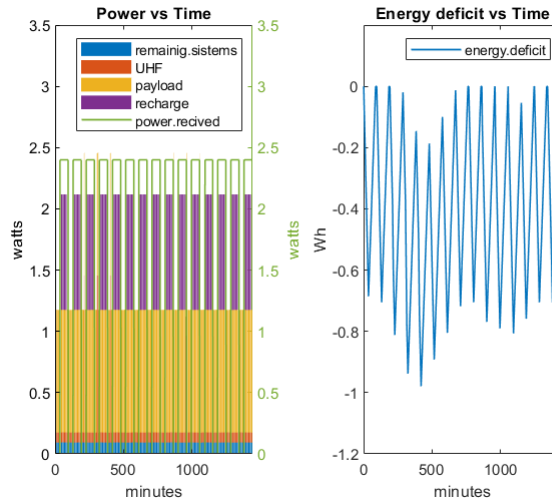


Figure 3.14. One day simulation with maximum eclipse time with time laps one minute, with alternative OBC.

3.3.4. Comparison among orbit RAANs

The table below (Table 3.1.) shows a summary about the different orbit RAAN analysis. It is right to say that the orbit with 0° RAAN (sun-synchronous) is the one with more power available and the best one in terms of energy available. But if we consider the traffic in the ground station, the 53.5° RAAN is the best option.

Table 3.1. Summary of the different orbit RAAN characteristics analyses

	0° RAAN	53.5° RAAN	90° RAAN
Maximum energy deficit in one orbit	0.683 Wh	0.821 Wh	0.918 Wh
Battery energy used in one year	596.5 Wh	3484 Wh	4064 Wh
Maximum eclipse time in minutes	24	31	36
Need change in the power consumption	no	no	yes
Passage in the Malpensa airport during the less traffic hours [1]	no	yes	no

4. Conclusion

From the analyses we can conclude that for the orbit planned for the mission (RAAN 53.5°), the projected satellite has enough power available to perform the mission without changing the algorithm of the power management.

The orbit with RAAN 0° is the orbit with more power available and is the best option if we do not consider the air traffic in the Malpensa airport during the communication time. However, considering the air traffic at the Malpensa airport the orbit with 53.5° RAAN is the best option and has enough power to perform the mission.

Only when we have orbits near the 90° RAAN the satellite has problems with the power available. In this case, the algorithm shall be changed to turn off the payload when the communication is on.

Also, some components can be changed to others with less energy consumption despite having less performance and needing adaptation to work with different components.

5. REFERENCES

- [1] SANZ CRISTÓBAL, J. A. (2018) Preliminary Orbital and Thermal Analysis of the ALSat#1 Mission. Corso di Laurea Magistrale in Ingegneria Spaziale. Facoltà di Ingegneria Industriale e dell'Informazione, Politecnico di Milano.
- [2] <https://www.industries-rd.it/home/index.php/en/dispositivi-elettronici-2/manufacturer>
- [3] Telescope Array project. The University of UTAH. USA. <http://www.telescopearray.org/>
- [4] De Angelis, A. (2012) Spontaneous Ionization to Subatomic Physics: Victor Hess to Peter Higgs. INFN Univ. Udine, INAF & LIP/IST Lisboa Spacepart CERN. Accessed online: https://www.google.pt/url?sa=t&rct=j&q=&esrc=s&source=web&cd=11&ved=2ahUKEwikxo6mkc3lAhWSHhQKHZPfAhsQFjAKegQIAhAC&url=https%3A%2F%2Ffindico.cern.ch%2Fevent%2F19779%2Fcontributions%2F371924%2Fattachments%2F291924%2F408037%2F12SpacepartDeangelis.pdf&usg=AOvVaw1ETy_b39Q47OUBfuafr-FS
- [5] https://www.researchgate.net/figure/Cosmic-ray-spectrum-E-3-over-10-orders-of-magni_fig1_24167401
- [6] Howell, E. (2018) What Are Cosmic Rays? Accessed online: <https://www.space.com/32644'-cosmic-rays.html>
- [7] Helvajian, H. and Janson, S.W. (2009) *Small Satellites: Past, Present and Future*. Chapter 1. The Aerospace Press, AIAA, Reston, VA, USA.
- [8] Foretscue, P., Swinerd, G. and Stark, J. (eds) (2011) *Spacecraft Systems Engineering*. (Fourth Edition) John Wiley sons, Ltd. United Kingdom. ISBN: 9780470750124
- [9] "CubeSat101 Basic Concepts and Processes for First-Time CubeSat Developers" (PDF), NASA CubeSat Launch Initiative, For Public Release - Revision Dated October (2017) accessed online: https://www.google.pt/url?sa=t&rct=j&q=&esrc=s&source=web&cd=1&ved=2ahUKEwjh38yok7XmAhWNEBQKHVAIC2sQFjAAegQIAxAC&url=https%3A%2F%2Fwww.nasa.gov%2Fsites%2Fdefault%2Ffiles%2Fatoms%2Ffiles%2Fnasa_csli_cubesat_101_508.pdf&usg=AOvVaw18_7kKiP0VuoAAFssq2vjo.
- [10] Helvajian, H. and Janson, S.W. (2009) *Small Satellites: Past, Present and Future*, Chapter 5. The Aerospace Press, AIAA, Reston, VA, USA.
- [11] <https://www.nanosats.eu/>
- [12] https://www.jpl.nasa.gov/news/press_kits/insight/launch/
- [13] <https://www.spacex.com/>

- [14] <https://www.nanosats.eu/ecosystem#suppliers>
- [15] Angrist, S. W. (1982) Direct Energy Conversion, Allyn and Bacon, New York, USA
- [16] [http:// https://sst-soa.arc.nasa.gov/](http://https://sst-soa.arc.nasa.gov/)
- [17] <https://batteryuniversity.com/learn>
- [18] Villela, T., Costa, C.A., Brandão, A.M., Fernando T. Bueno, F.T. and Leonardi, R. (2019) Towards the Thousandth CubeSat: A Statistical Overview. International Journal of Aerospace Engineering, Volume 2019, Article ID 5063145, 13 pages, <https://doi.org/10.1155/2019/5063145>
- [19] <https://www.endurosat.com/products/>
- [20] Veerendra (2017) Relationship between Energy Transferred, Current, Voltage and Time. Accessed online: <https://www.aplustopper.com/relationship-energy-transferred-current-voltage-time-power/>
- [21] https://www.google.pt/url?sa=t&rct=j&q=&esrc=s&source=web&cd=1&cad=rja&uact=8&ved=2ahUKEwjmwLfego3lAhXpylUKHey_CJUQFjAAegQIARAC&url=https%3A%2F%2Fwww.endurosat.com%2Fmodules-datasheets%2FEPS_User_Manual_Rev_2.pdf&usg=AOvVaw1Du-Plfk0qSlHcijAeCM1d
- [22] <https://www.mpoweruk.com/soc.htm>
- [23] https://www.google.pt/url?sa=t&rct=j&q=&esrc=s&source=web&cd=2&cad=rja&uact=8&ved=2ahUKEwiq4b7rh43lAhUDaBoKHd61BTMQFjABegQIAhAC&url=https%3A%2F%2Fwww.endurosat.com%2Fmodules-datasheets%2FUHF_type_II_Datasheet_Rev_1.6.pdf&usg=AOvVaw3esqWDnQcwm7LJoZIOx8k4
- [24] <https://www.st.com/en/microcontrollers-microprocessors/stm32f4-series.html>
- [25] https://www.google.pt/url?sa=t&rct=j&q=&esrc=s&source=web&cd=2&cad=rja&uact=8&ved=2ahUKEwi_pda74-XmAhXlzoUKHQzLB_QQFjABegQIAhAC&url=https%3A%2F%2Fwww.endurosat.com%2Fmodules-datasheets%2FOBC_Datasheet_Rev1.pdf&usg=AOvVaw17vNUbl1oXOwfGOSrvEenC
- [26] <https://www.techopedia.com/definition/24481/flash-memory>
- [27] http://ww1.microchip.com/downloads/en/DeviceDoc/atmegas128_ds.pdf
- [28] http://ww1.microchip.com/downloads/en/DeviceDoc/ATmegaS64M1_datasheet_ds60001506b.pdf
- [29] https://www.google.pt/url?sa=t&rct=j&q=&esrc=s&source=web&cd=11&cad=rja&uact=8&ved=2ahUKEwiahv2ijpflAhX1AWMBHR99AtwQFjAKegQIABAC&url=https%3A%2F%2Fwww.endurosat.com%2Fmodules-datasheets%2FATmegaS64M1_datasheet_ds60001506b.pdf&usg=AOvVaw17vNUbl1oXOwfGOSrvEenC

at.com%2Fmodules-

datasheets%2FUHF_Antenna_III_Datasheet_Rev1.pdf&usg=AOvVaw1bMssN6x_x873RnihSb-Eo

[30]<https://www.google.pt/url?sa=t&rct=j&q=&esrc=s&source=web&cd=11&cad=rja&uact=8&ved=2ahUKEwjo47O1lZflAhXjxoUKHfxlAcoQFjAKegQIBRAC&url=https%3A%2F%2Fwww.endurosa.com%2Fmodules->

datasheets%2FSolar%2520Panel_1U_Datasheet_Rev1_5.pdf&usg=AOvVaw1kSts8aVqBv_FvvMSheaCd

[31]https://www.google.pt/url?sa=t&rct=j&q=&esrc=s&source=web&cd=1&ved=2ahUKEwipnJj2tbrmAhWOGBQKHesrCFkQFjAAegQIARAC&url=https%3A%2F%2Fwww.cesi.it%2Fservices%2Fsolar_cells%2FDocuments%2FCTJ30-2015.pdf&usg=AOvVaw3UFdFLEITRB_qXk3YarY0e

[32] Suparta, W., Zulkeple, S.K. (2018) Investigating Space Radiation Environment Effects on Communication of Razaksat-1. *J Aersp Technol Manag*, 10: e2218, doi: 10.5028/jatm.v10.815

[33] https://pages.mtu.edu/~raman/SilverI/MiTEP_ESI-2/Solar_Constant.html